Supplementary Information (SI)

Supplementary figures

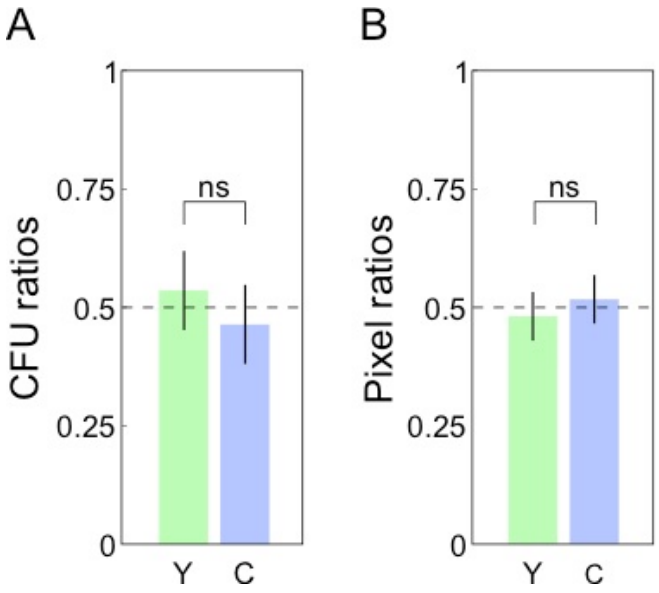

Figure S1: (A) Colonies were scraped from the agar plates after 14 days of growth, and CFUs of each strain counted. The plot shows the overall ratios from all colonies. (B) Ratios are total green or blue pixels in all colony images on day 14. The ratios in both methods were not significantly different from 0.5 (sign test, both $P > 0.05$).

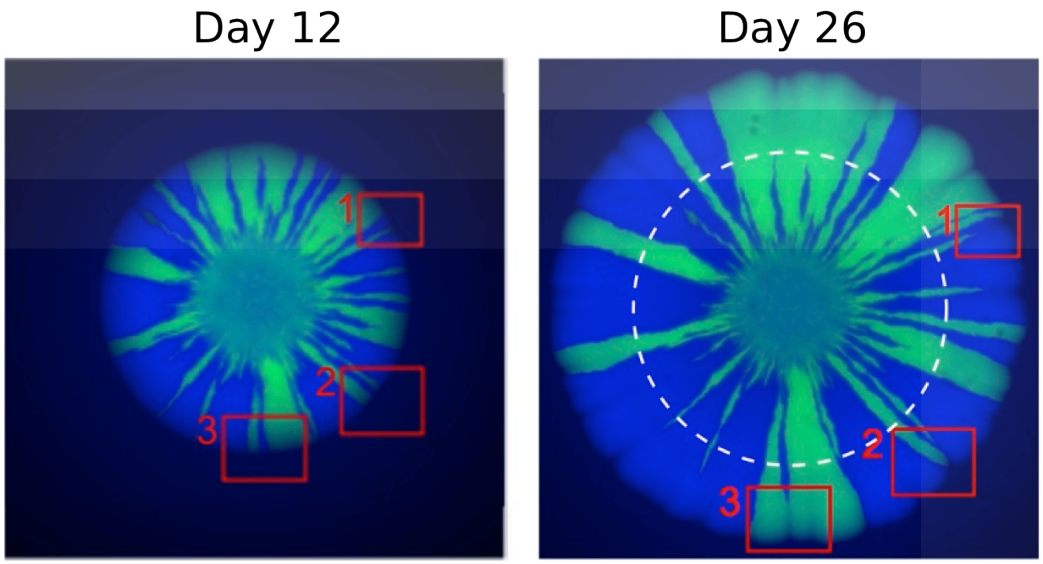

Figure S2: Same colony at nutrient level 0.15 on day 12 and day 26. Numbered boxes show corresponding examples of where sectors in the day 12 colony were pinched off by mutants that had arisen by day 26. We therefore analyse all data on day 12 (dashed circle in the day 26 colony) to minimise the effect of mutations.

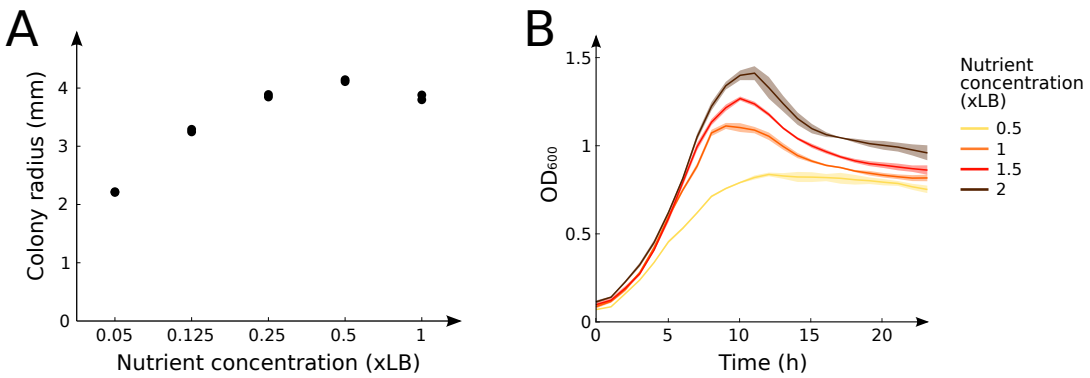

Figure S3: Justifying the choice of nutrient concentrations. (A) Colony radii on day 6 at different nutrient concentrations (2 replicates). Varying nutrient concentration in agar plates revealed that colony radius increased linearly up to a concentration of 0.25xLB, above which colonies remained approximately the same size or even decreased in size. (B) OD_{600} of YFP strain growing in liquid over 24 hours at different nutrient concentrations grown at 37°C, where measurements were taken every hour. Shaded areas show standard deviations between 3 replicates. At nutrient concentrations of 0.5xLB and higher, optical densities go down after the nutrients have been exhausted. This is presumably due to changes in pH (Heurlier et al., 2005). For these reasons, we focused our experiments on the range of 0.025x to 0.2x.

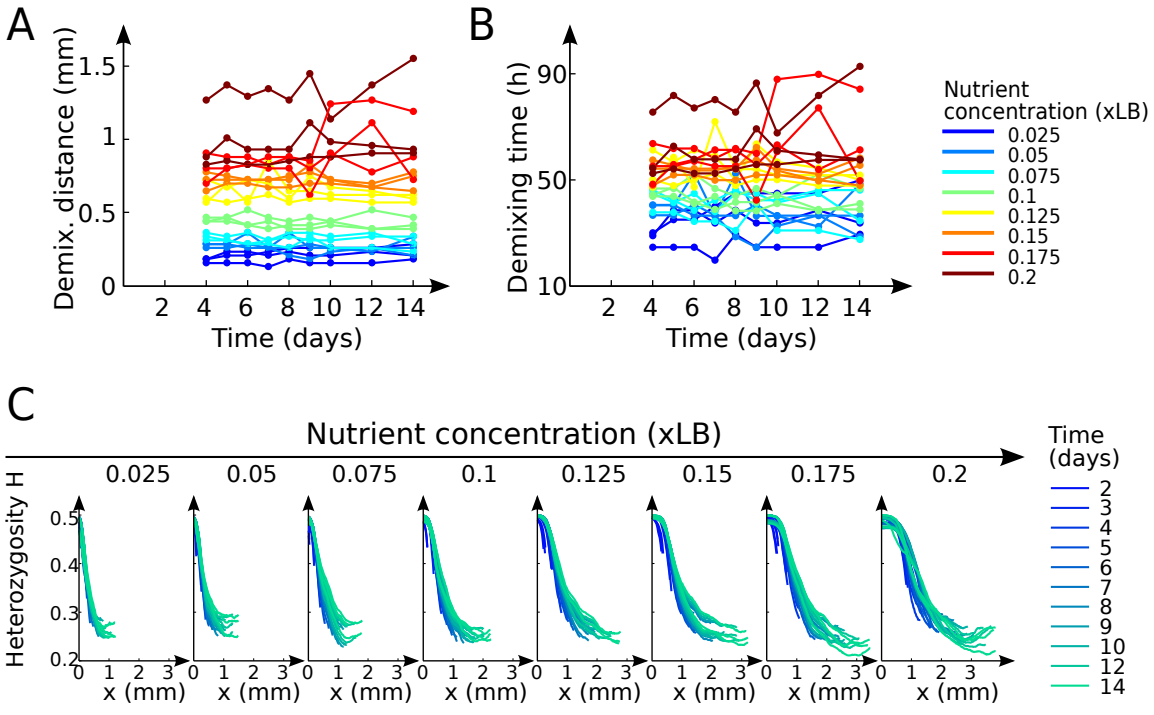

Figure S4: Demixing changes very little over time. (A)-(B) Demixing points in space and time did not follow a significant slope between pictures taken on days 4 to 14 (GLM for demixing distance P = 0.33). Before day 4, some of the colonies had not demixed, so data was not used. This shows that once the two strains had demixed, they remained so. (C) Heterozygosity H as a function of inoculum distance x was calculated for each colony from pictures taken on different days. Each nutrient concentration is represented by images from three replicate colonies. The curves at each nutrient concentration fall approximately on top of each other, showing that H remains approximately the same between measurements.

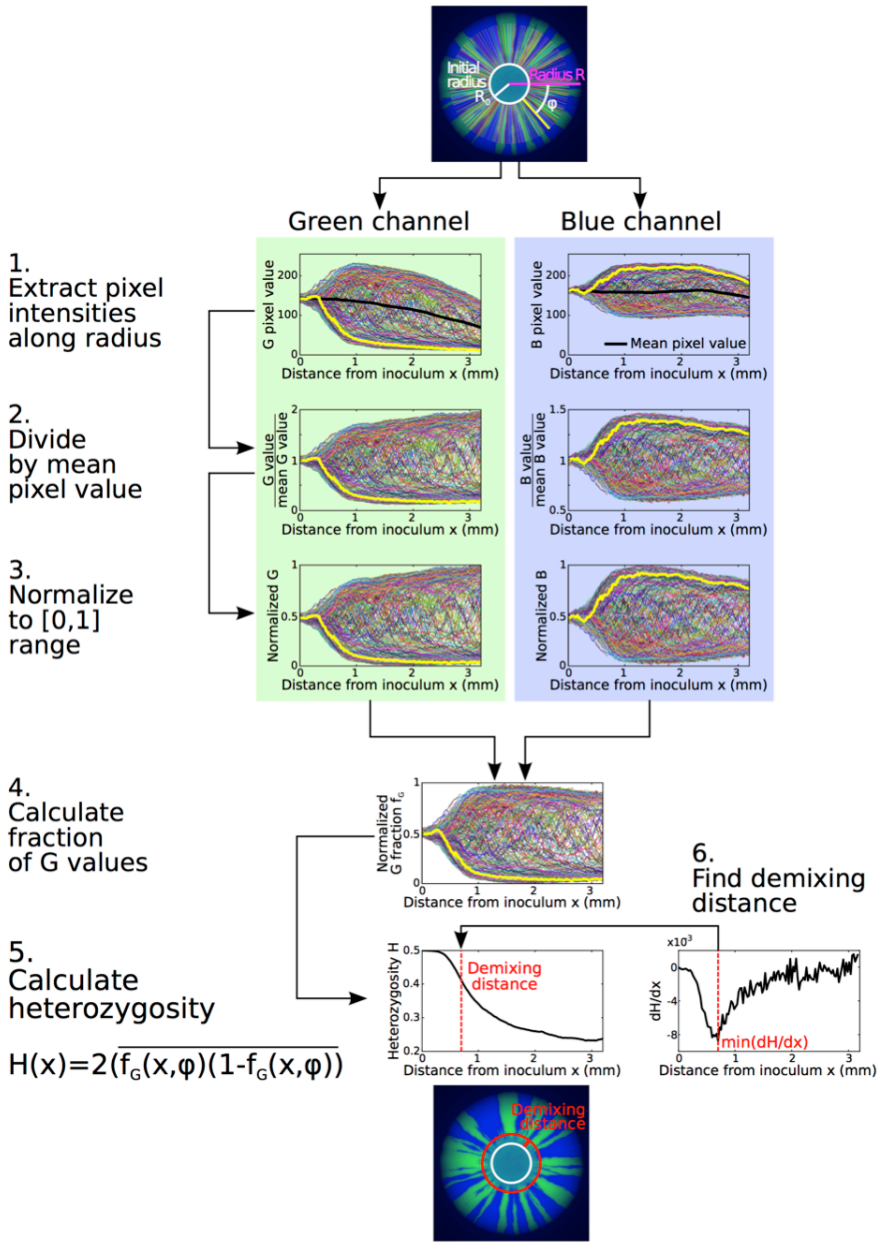

35

36 **Figure S5:** How to calculate heterozygosity index H. (1) Lines were drawn on each
37 colony starting from the inoculum and extending outward to 85% of the colony
38 radius (beyond that, the colony got darker due to its 3D structure, making it difficult
39 to distinguish green and blue) at angles ϕ around the center between [−π..π]. We
40 then extracted the green and blue pixel intensities along each line at angles ϕ and
41 steps of 2 pixels away from the inoculum. (2) Because the range of pixel intensities

changed with increasing distance x from the inoculum, and because it differed between green and blue, we divided all pixel values by the mean intensity at the corresponding distance from the inoculum. (3) These values were then normalized separately for green and blue to a [0..1] range using the following equation: $(p(x, \phi) - p_{min})/(p_{max} - p_{min})$ where $p(x, \phi)$ is the pixel value at distance x from the inoculum and angle ϕ, and p_{max} and p_{min} are the maximum and minimum intensities over all values of p in the whole colony. (4) We then calculated the relative intensity of green f_G at each distance x and angle ϕ as: $f_G(x, \phi) = p_G(x, \phi)/(p_G(x, \phi) + p_B(x, \phi))$ where p_G are p_B are the normalized green and blue values described in step 3. (5) We calculated H for each distance x as: $H(x) = 2\left[\sum_{\varphi} f_G\,(x, \varphi)\big(1 - f_G(x, \varphi)\big)\right]/\Phi$, where Φ is the number of angles sampled around the circumference (here $\Phi = 315$). (6) The demixing distance was then determined by finding the distance at which the first derivative of H (dH/dx) was minimal. The logic behind this is that until that point, the two strains are increasingly demixing and after that point, the pattern begins to converge on its final sector number S. Plots (in Fig. 2) show H as a function of distance, which is obtained as described above, and as a function of time, which is calculated by dividing the distance x-axis by each colony's radial expansion velocity v.

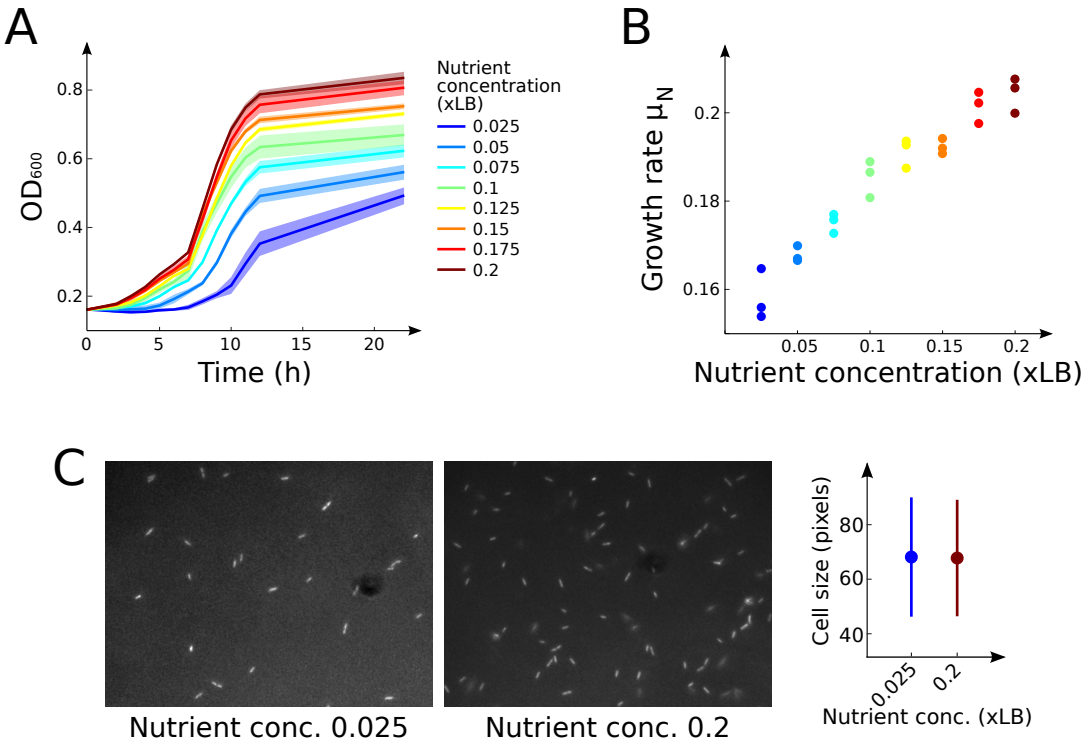

Figure S6: Estimating growth rates μ based on growth in liquid at nutrient concentrations N. (A) OD_{600} of YFP strain growing in liquid at 22°C over 24 hours at different nutrient concentrations. Measurements were taken every hour for the first 12 hours and once at 24 hours. Shaded areas show standard deviations between 3 replicates. These growth curves were used to estimate growth rates μ_N, shown in panel (B) by computing the slope between the OD_{600} values at 0 and 12 hours (see SI text 2). (C) Because OD_{600} values depend on cell size, we have verified that cell sizes do not differ significantly between the highest and lowest concentration of LB (P=0.91).

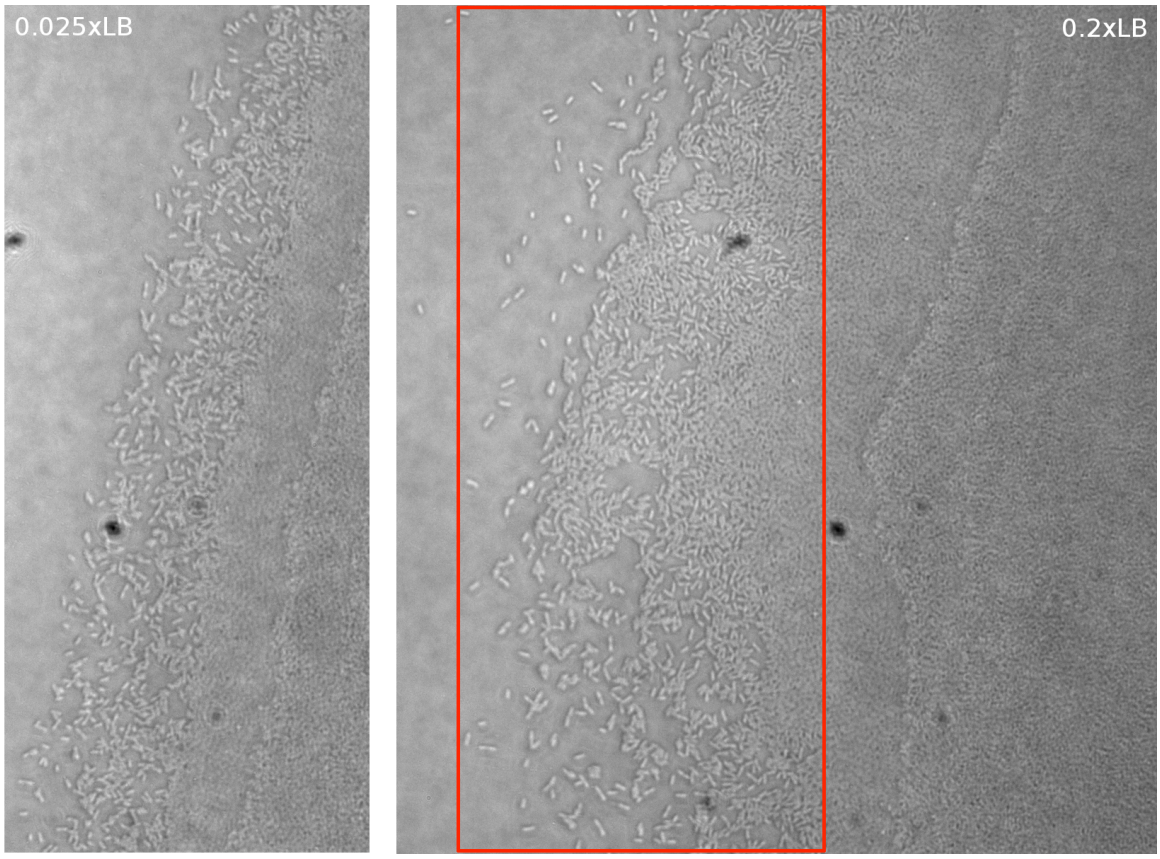

Figure S7. Cell size does not change with nutrient concentration. Brightfield images of a colony edge at nutrient concentrations 0.025x and 0.2x LB. Image processing to automatically measure cell size in the left image and the section of the image within the red box on the right revealed that there was no significant difference between cell size (mean ± sd: 61.85 ± 16.21 and 63.02 ± 16.05 for 0.025x and 0.2x, respectively, Mann-Whitney test: P=0.33).

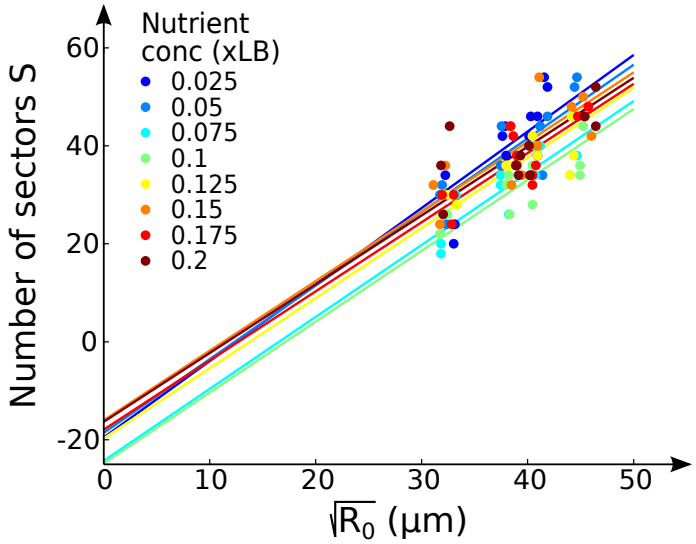

Figure S8: Estimating D_g from S, D_s and R_0. According to equation 2, by plotting sector number S against $\sqrt{R_0}$, we can fit lines through these points with slope $H_0\sqrt{2\,\pi v/D_s}$ and y-axis intersection $2\pi H_0\, v/D_g$. D_g could then be calculated from the y-axis intersection.

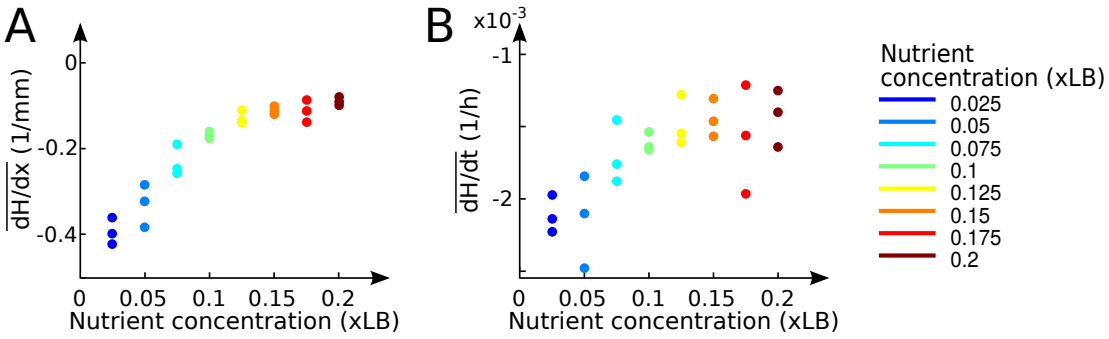

Figure S9: Change in Heterozygosity H in colonies. (A) The average of the slope of H measured over distance x from the inoculum for all datapoints between x = 0 and the demixing distance on day 12. (B) The average of the slope of H measured over time t for all datapoints between t = 0 and the demixing time, calculated on day 12 colonies.

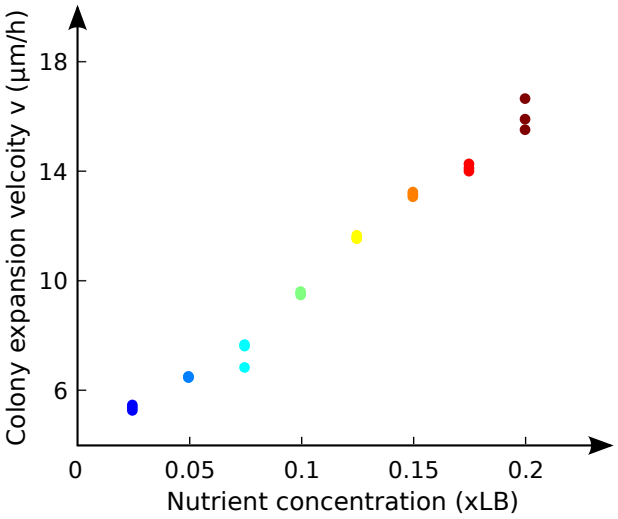

Figure S10: Colony expansion velocity v as a function of nutrient concentrations.

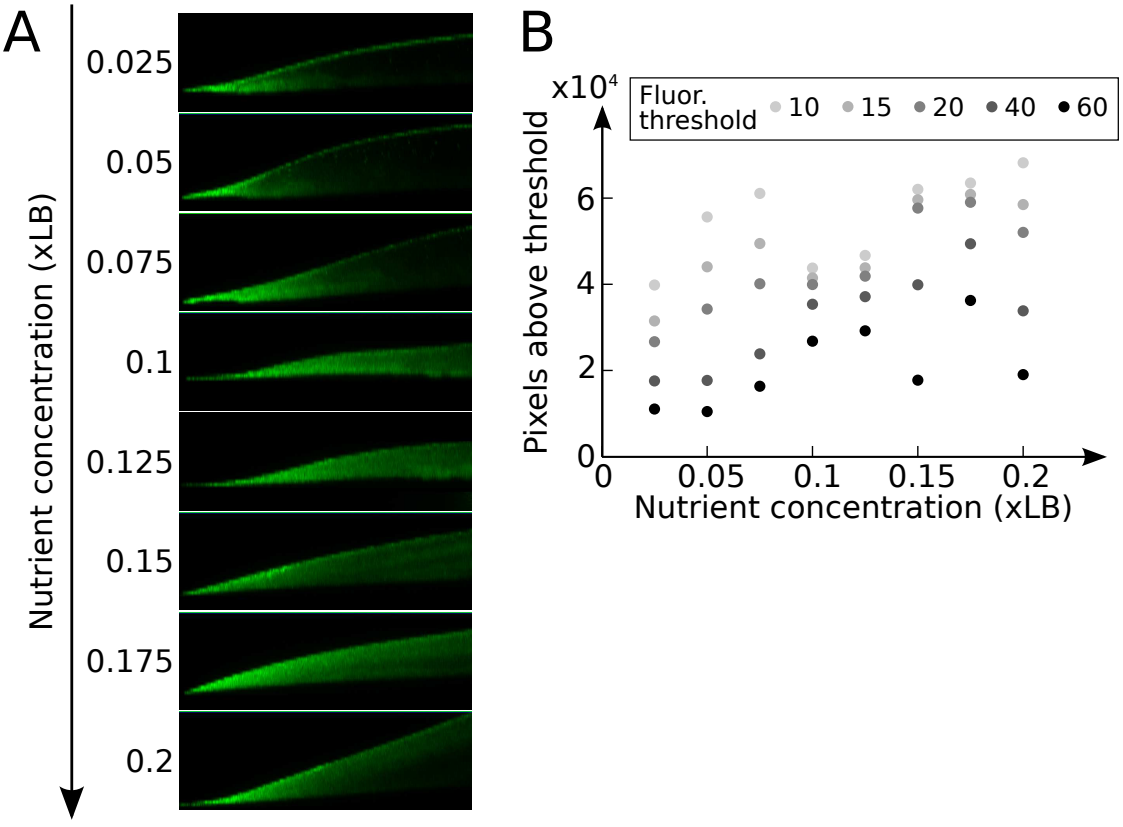

Figure S11: (A) Confocal images of rrn colonies at different depths on day 6. One replicate was imaged for each nutrient concentration. (B) Number of pixels above a given fluorescence threshold in each of the images in panel A. At all thresholds

except 60, nutrients and pixels were significantly positively correlated (Spearman's $0.74 < \rho < 0.9$, $P < 0.05$, at threshold 60: $\rho = 0.71$, $P = 0.058$).

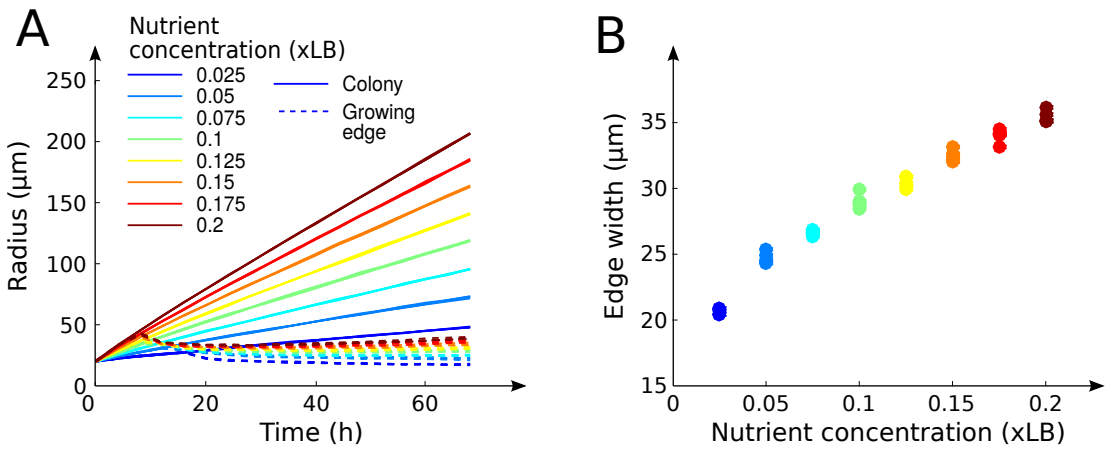

Figure S12: (A) Radii of the simulated colonies, together with the width of the edge containing growing cells. Colony radius was calculated as the average of the distances between the furthest two cells from the center in both the x and y dimensions. (B) Growing edge width as a function of nutrient concentration. This width was calculated as the radius of the colony minus the radius of the area containing all grid elements whose nutrient concentration was lower than 0.01.

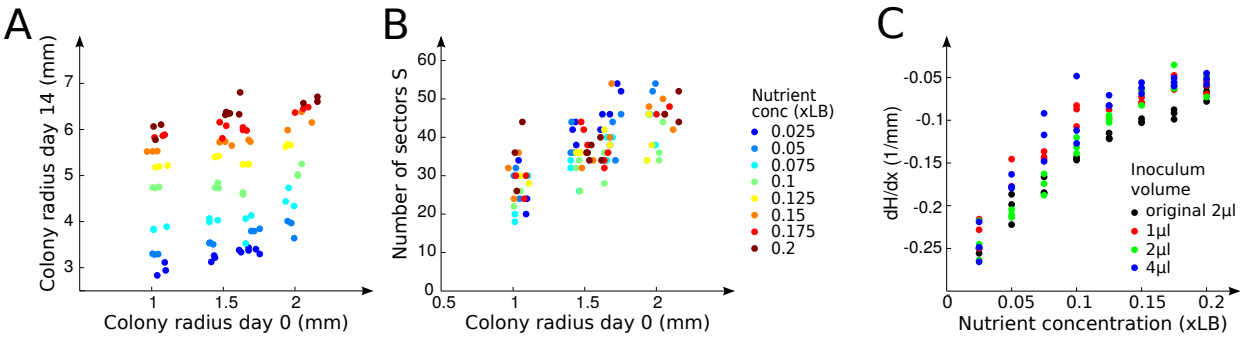

Figure S13: Effects of changing initial radii R_0. (A) Final colony radius after 14 days as a function of initial inoculum size. Colonies were larger with larger inoculum sizes.

(B) Number of sectors on day 14 as a function of initial inoculum size. Larger inocula resulted in more sectors, but sector number does not vary significantly with nutrients. (C) dH/dx is not significantly affected by R_0 ($P = 0.9$), but is significantly affected by nutrient concentrations ($P < 0.001$).

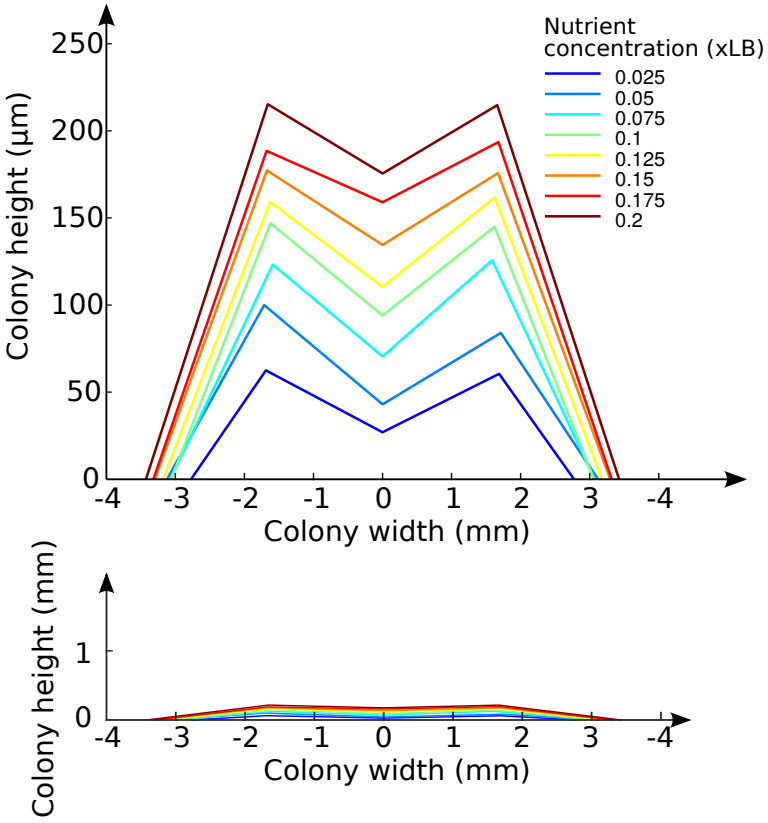

Figure S14: Height of colonies, estimated using confocal microscopy, measuring five points along the widest part of the colony. Values of the x-axis were determined by the 2D measurements of the colony radius, and the highest points were set to be at the initial inoculum radius, where we expect the so-called "coffee-ring effect" of the dried inoculum to result in higher cell concentrations at the edge of the drop. The bottom plot shows the same data but scaled to match each other.

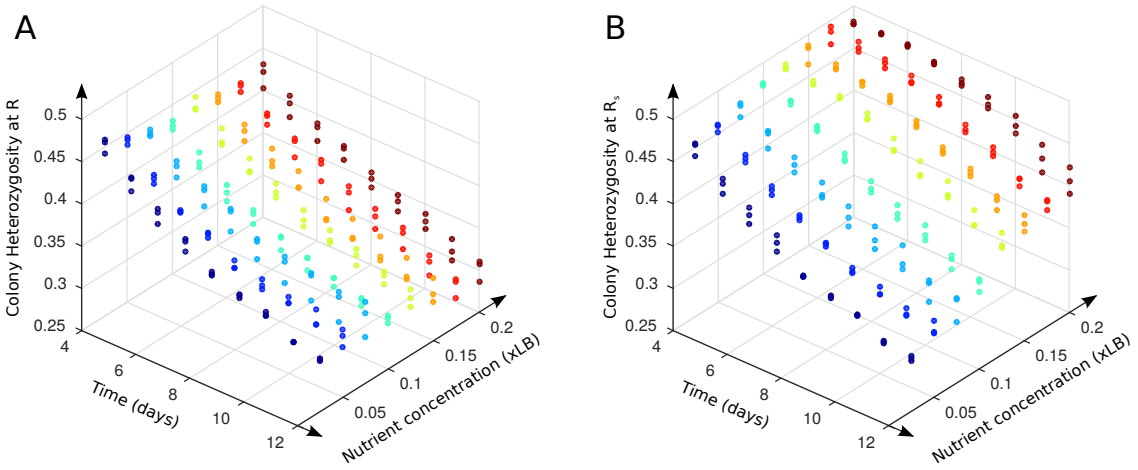

117

118 **Figure S15:** Colony heterozygosity CH measures strain diversity over the whole
119 colony. (A) CH is calculated by taking the whole colony, up to the edge of the colony
120 R (time-controlled). (B) CH is calculated by taking only part of the colony (from the
121 center to R_s) where R_s is the radius of the smallest colony on that day across nutrient
122 concentrations (size-controlled). The x-axis shows the day on which the colony
123 pictures were taken and the y-axis shows nutrient concentrations. The plot shows
124 that size-controlled CH increases with increasing nutrient concentrations, following
125 the patterns observed for demixing distance, regardless of the day it is measured on,
126 while time-controlled colonies do not vary much, consistent with changes in dH/dt
127 with nutrients.

128

129 **Supplementary text 1.** In the main text, we describe experiments to visually quantify
130 the width of the growing edge. The data from these experiments are qualitative,
131 however, because the fluorescent protein is known to have a half-life of
132 approximately 24 hours (Andersen et al., 1998), such that cells will continue to
133 fluoresce after they have stopped growing. In addition, colonies became thicker with

increasing nutrients (Fig. S14), leading to a higher cumulative fluorescence when colonies were observed from the top. We therefore also used confocal microscopy to measure the fluorescence intensities at different depths at the edge of the colonies. These data support our findings that the area at the edge of the colonies in which cells are growing correlates positively with nutrient concentrations (Spearman's $\rho = 0.9$, $P < 0.005$ between nutrient concentration and number of pixels with values above 20, Fig. S11).

Supplementary text 2: Detailed Materials & Methods

Bacterial strains and isolates. The following bacterial strains were used in this study: *P. aeruginosa* PA4, PAO1 wild-type (WT), pili mutants (ΔpilB) and PAO1 wild-type with an rRNA transcriptional GFP fluorescent reporter built in (rrn). The wild-type PAO1 strain was kindly provided by Roberto Kolter and the knock-out strain constructed by a clean deletion of the *pilB* gene. The *P. aerugionsa* rrn strains were generously provided by Phil Stewart, who inserted an rrnBp1-GFP-AGA plasmid into a PAO1 background.

Cultures and growth conditions

LB agar plates were prepared at 8 different concentrations of LB-Miller, starting at 0.025x and increasing in steps of 0.025x to 0.2x. We did this by increasing the concentrations of yeast extract (0.125g/l – 1g/l) and tryptone (0.25g/l – 2g/l), while holding agar and NaCl concentrations constant at 15g/l and 10g/l, respectively. Each plate contained 25ml of 1.5% LB agar and plates were left to dry (lids on) overnight

156 at room temperature.

157 Liquid cultures of each strain were incubated at 37°C and constantly shaken (250
158 rotations per minute) overnight in 3ml of 1x LB broth. Fresh 3ml aliquots of 1x LB
159 were then reseeded with the overnight cultures to an OD_{600} = 0.05 and grown for 2
160 hours at 37°C, constantly shaken. The YFP and CFP-tagged cultures were then mixed
161 at a 1:1 ratio in phosphate buffer solution (PBS), resulting in a 1ml mixture at OD_{600} =
162 0.3. The rrn cultures were simply diluted to an OD_{600} = 0.3 in PBS to a total of 1ml.
163 2µl of the two-strain mixture, or the rrn culture, were then spotted onto each agar
164 plate, left to dry (until the drop was no longer visible) and then turned over. In the
165 experiment where the initial inoculum radius was varied, drops of either 1µl, 2µl or
166 4µl were deposited onto the agar. All colonies were left to grow on overturned
167 plates for 14 days at room temperature (22°C).

168 **Imaging and image analysis.** Colonies were imaged using a stereoscope (Zeiss Lumar
169 V.12), a 0.5x objective, at zoom 3.5x. Fluorescence exposure (YFP and CFP filter sets)
170 was automatically adjusted for the mixed colonies and fixed to 150ms for the rrn
171 colonies (YFP). Images were taken 1 hour after the colonies had dried (using dark
172 field light), and then every 24 hours for the first 10 days, and subsequently every 48
173 hours.

174 All image analysis was conducted using MatLab R2010a. Colony radii at day 0 (R_0)
175 were measured manually. After that, tools provided by the MatLab Image Processing
176 toolbox were used to automatically trace a line around each colony, (parameters
177 were fixed through trial and error to yield good estimates of the colony radii). The
178 distances of each point on the edge of the colony to the central point were then

averaged to yield the colony radius.

Estimating experimental parameters. To calculate μ_N for each nutrient concentration used in the agar plates ($0.025 < N < 0.2$), *P. aeruginosa* cells were grown in 150µl of shaken liquid culture containing the corresponding nutrient concentration in a 96-well plate. These cultures were inoculated with cells that had been grown overnight, diluted to an OD_{600} of 0.05, grown for an additional 2 hours, and subsequently diluted down to an OD_{600} of 0.05 to ensure that cells were in the exponential growth phase. Growth rate μ_N was calculated as follows:

$$\mu_N = \frac{log_2(OD_{N,t_2}/OD_{N,t_1})}{t_2 - t_1} \quad (2)$$

where t_1 = 0h and t_2 = 12h and $OD_{N,t}$ was the average OD_{600} of three replicate cultures at time t and nutrient concentration N. OD_{600} was measured using a 96-well plate in a Tecan Infinite® 200 PRO microplate reader. Growth rates were estimated using YFP cells (Fig. S6) due to the noise in the CFP values.

Heterozygosity H was measured using the following algorithm (visualized in Fig. S5): (1) Lines were drawn on each colony starting from the inoculum and extending outward to 85% of the colony radius (beyond that, the colony got darker due to its 3D structure, making it difficult to distinguish green and blue) at angles ϕ around the center between $[-\pi..\pi]$. We then extracted the green and blue pixel intensities along each line at angles ϕ and steps of 2 pixels away from the inoculum. (2) Because the range of pixel intensities changed with increasing distance x from the inoculum, and because it differed between green and blue, we divided all pixel values by the mean intensity at the corresponding distance from the inoculum. (3)

These values were then normalized separately for green and blue to a [0..1] range using the following equation: $(p(x, \phi) - p_{min})/(p_{max} - p_{min})$ where $p(x, \phi)$ is the pixel value at distance x from the inoculum and angle ϕ, and p_{max} and p_{min} are the maximum and minimum intensities over all values of p in the whole colony. (4) We then calculated the relative intensity of green f_G at each distance x and angle ϕ as: $f_G(x, \phi) = p_G(x, \phi)/(p_G(x, \phi) + p_B(x, \phi))$ where p_G are p_B are the normalized green and blue values described in step 3. (5) We calculated H for each distance x as:

$$H(x) = 2\left[\sum_{\varphi} f_G\,(x, \varphi)\big(1 - f_G(x, \varphi)\big)\right]/\Phi \qquad (3)$$

where Φ is the number of angles sampled around the circumference (here $\Phi = 315$). (6) The demixing distance was determined by finding the distance at which the first derivative of H (dH/dx) was minimal.

The overall colony heterozygosity CH was used to estimate a different property: the likelihood of a cell at an arbitrary place in the colony to be in a clonal patch. We excluded the inoculum area, since its size is arbitrary. Rather than sampling points along the radii of the colony as for heterozygosity H, we instead sampled pixels at equidistant points around circumferences at steps of 2 pixels from the inoculum, leading to a set of Z evenly distributed points. As for H, we extracted the green and blue pixel intensities at each point z, divided all pixel values by mean intensity of all Z points, normalized them to a range of [0..1] $(p(z) - p_{min})/(p_{max} - p_{min})$ where p(z) is the pixel value at point z, and calculated the relative green intensity as: $f_G(z) = p_G(z)/(p_G(z) + p_B(z))$ where p_G are p_B are the normalized green and blue values. CH was calculated as follows:

$$CH(x) = 2\left[\sum_{z=1}^{Z} f_G\,(z)\big(1 - f_G(z)\big)\right]/Z \quad (4).$$

For a time-controlled measure of CH, we took all points Z reaching from the inoculum all the way to the outside of the colony at that time-point (e.g. day 12). For the size-controlled measure, we determined the radius of the smallest colony at that time-point (e.g. day 12) and for each colony used all points Z between the inoculum and that radius to calculate CH.

N_e was calculated using the following equation:

$$N_e = \frac{wh_e w_c}{2V_c} \quad (5)$$

where w is the width of the growing edge, w_c the width of a single cell (here w_c = 1µm), h_e is the height of the colony at the inner point of the growing edge, and V_c is the volume of a single cell (here V_c = 1µm^3). To estimate h_e, we first drew a line from the highest point in the colony (measured using confocal microscopy as described below, and assumed to be at a distance x = R_0 from the center) to the colony edge (at height 0). We then calculated the height of the line at distance R − w from the colony center.

The genetic diffusion constant D_g is inversely proportional to N_e where γ is some constant (Korolev et al., 2010, Nei et al., 1975):

$$D_g = \frac{\gamma}{N_e} \quad (7).$$

D_g could also be estimated from equation 2, using the estimates of R_0, D_s and S. By plotting sector number S against $\sqrt{R_0}$, we can fit lines through these points

with slope $H_0\sqrt{2\,\pi v/D_s}$ and y-axis intersection $2\pi H_0\; v/D_g$ (Fig. S8).

The cellular diffusion rate D_s was estimated by analyzing the edges between the sectors in the colonies. Edges between sectors were found automatically using an edge detection package developed by Peter Kovesi (Kovesi). We applied this algorithm at a distance $R_0 < R < 0.95\ R_c$ from the center, where R_c is the colony radius and R_0 is the initial inoculum radius. This allowed us to avoid detecting the colony edge, and thousands of small edges in the initial inoculum area. Edges shorter than 15 pixels (194.8μm) were discarded to avoid well-mixed areas, particularly close to the center. This method did not detect all sector edges, but was reliable in detecting edges between well-formed sectors (Fig. 6B). For each point along each edge between sectors, we measured the distance R from the center and angle α from a horizontal line drawn through the center of the colony, and estimated var(α), the variance of the angles along the edge and the distance between the $1/R_i$ and $1/R_f$, where R_i is the distance between the colony center and the closest point on the edge, and R_f the furthest point. Using the following equation:

$$var(\alpha) = \frac{2D_s}{v}\left(\frac{1}{R_i} - \frac{1}{R_f}\right) \qquad (6)$$

we could then estimate $2D_s/v$ as the slope of the regression line between var(α) and $1/R_i - 1/R_f$ (Fig. 6). Datapoints were then binned together based on their $1/R_i - 1/R_f$ value (bin size 8×10^{-5}) and the mean value of var(α) for all points in each bin was used to calculate the linear regression. All points whose var(α) value fell further than 3 standard deviations away from the mean of the points in the bin were discarded, since they were thought to be cases where the algorithm failed at adequately

detecting edges. This reduced the noise in the fit without changing the qualitative result. A point through the origin was included in the linear regression fit for each nutrient concentration.

Confocal laser scanning microscopy (CLSM) was conducted using an LSM 700 laser scanning inverted confocal microscope (Zeiss). Squares of agar were cut around the colony, which was placed on a microscope slide for imaging. ΔpilB colonies were imaged with automated exposure, whereas rrn colonies were imaged at a fixed exposure 150ms. One ΔpilB colony (nutrient concentration 0.2x on day 7) was imaged along the edges of a sector using a 50x objective to verify that patterns at the surface were representative of cells growing deeper below the surface (Fig. 1D). 3D images were rendered using the Zen Black software. rrn colonies were used to determine the level of fluorescence at the edge, and to calculate colony profiles along the z-axis. This was done by imaging the edge of each colony with slices 2µm apart along the z-axis, and, moving sideways along the colony diameter, also imaging the highest point in the colony, the center, the next highest point and the opposite edge. By using the heights of the highest slice within these five measurements, we could estimate the profile of the colony (Fig. S14).

Computational model. Compared to previously published studies using this model, the initial positioning of the cells and the boundary conditions were as follows: 200 cells were placed at the center of a square space, containing nutrients at a given concentration (0.375x, x = [1, 2, .., 8]). When nutrient gradients were allowed to form, each cell's growth reduced the concentration of nutrients in its grid element. Grid elements containing no cells (e.g. at the outside of the square) were kept at a

constant concentration of nutrients, which could diffuse toward other grid elements. When nutrient gradients were off, nutrient concentrations were simply kept constant in all grid elements.

Compared to previous publications, we also modified the following parameters: maximum growth rate μ_{max} was changed from 1 to 1.0152 (as experimentally measured, see below), the half-saturation constant for nutrient concentration K_N was changed from 3.5×10^{-5} to 1.5 (as experimentally measured), nutrient diffusion was reduced from $4 \times 10^4 \mu m^2/h$ to $200 \mu m^2/h$ such that gradients could form at the edges relatively soon (this was adjusted by trial an error to obtain results that were qualitatively similar to the real colonies), and the duration of each run, which was fixed to 72 hours in the runs with nutrient gradients (chosen to reveal differences between the colonies). In runs with no gradients, simulations were stopped when the same biomass as the corresponding gradient simulations had been reached. Stoichiometry equations describing cell metabolism were as in Table S2 in ref. (Mitri et al., 2011). Even though some parameters were estimated experimentally, comparisons with the experimental data should only be qualitative.

Simulated colony analysis. Colony radius R was calculated as the average of the distances between the furthest two cells from the center in both the x and y dimensions. The width of the growing edge w was calculated as the radius of the colony minus the radius of the area containing all grid elements whose nutrient concentration was lower than 0.01.

To calculate heterozygosity H for simulated colonies, the region of the colony beyond the initial inoculum was divided into bands of 5μm width, at increasing

distances x from the inoculum. In each band, 22 equidistant points were marked around the circumference, and a box of width 5µm × 5µm sampled around each point. The number of green and blue cells were then counted in each of these sections to yield the proportion of green cells f_G. We then used equation 3 to compute H by averaging over sections sampled in each band. The demixing distance was determined – as in the experiments – as the point in space where the maximum magnitude of the slope of H was reached.

Estimating simulation parameters. The maximum growth rate μ_{max} used in the simulations was estimated experimentally as for μ_N (see above) in a liquid culture containing 2xLB (N=2). This value was found to be 1.0152 cell division per hour. K_N was computed by fitting a Monod curve through the estimated growth rates at different nutrient concentrations (μ_N and μ_{max}) using the Matlab curve fitting tool. The fit estimated that half the maximum growth rate was reached at 0.1xLB.

Nutrient concentrations in the simulations ranged from 0.375 to 3 in steps of 0.375. This was based on the total concentration of yeast extract and tryptone in g/l, such that 0.025xLB corresponded to 0.125g/l of yeast extract and 0.25g/l of tryptone (total: 0.375) and 0.2xLB was taken to contain a tota l nutrient concentration of 3g/l.

References

Andersen JB, Sternberg C, Poulsen LK, Bjorn SP, Givskov M & Molin S. (1998). New unstable variants of green fluorescent protein for studies of

transient gene expression in bacteria. Applied and environmental microbiology 64**:** 2240-6.

Heurlier K, Haenni M, Guy L, Krishnapillai V & Haas D. (2005). Quorum-sensing-negative (lasr) mutants of pseudomonas aeruginosa avoid cell lysis and death. Journal of bacteriology 187**:** 4875-4883.

Korolev KS, Avlund M, Hallatschek O & Nelson DR. (2010). Genetic demixing and evolution in linear stepping stone models. Reviews of modern physics 82**:** 1691-1718.

Kovesi PD Matlab and octave functions for computer vision and image processing. Centre for Exploration Targeting, School of Earth and Envrionment, The University of Western Australia.

Mitri S, Xavier J & Foster K. (2011). Social evolution in multispecies biofilms. PNAS 108**:** 10839-46.

Nei M, Maruyama T & Chakraborty R. (1975). The bottleneck effect and genetic variability in populations. Evolution 29**:** 1-10.